Nuclear Inst. and Methods in Physics Research, A 993 (2021) 165080

Contents lists available at ScienceDirect

Nuclear Inst. and Methods in Physics Research, A

journal homepage: www.elsevier.com/locate/nima

Nitrogen doping with dual-vacuum furnace at IHEP

Baiqi Liu [a,b,c], Peng Sha [a,b,c,*], Chao Dong [a,b,c,**], Feisi He [a,b,c], Weimin Pan [a,b,c,d], Zhenghui Mi [a,b,c], Jiyuan Zhai [a,b,c], Song Jin [a,b,c], Jin Dai [a,b,c], Zhongquan Li [a,b,c], Lei Du [a,b,c], Fei Wang [a,b,c,d], Liangrui Sun [a,b,c], Rui Ge [a,b,c]

[a] Institute of High Energy Physics, Chinese Academy of Sciences, Beijing 100049, China
[b] Key Laboratory of Particle Acceleration Physics & Technology, Institute of High Energy Physics, Chinese Academy of Sciences, Beijing 100049, China
[c] Center for Superconducting RF and Cryogenics, Institute of High Energy Physics, Chinese Academy of Sciences, Beijing 100049, China
[d] University of Chinese Academy of Sciences, Beijing 100049, China

ARTICLE INFO

Keywords:
Nitrogen doping
Superconducting cavity
Quality factor
Gradient
Dual-vacuum furnace

ABSTRACT

A dual-vacuum furnace with the heater in the outside vacuum has been developed at the Institute of High Energy Physics (IHEP) to perform nitrogen doping (N-doping) heat treatment of 1.3 GHz 1-cell niobium cavity. The inner chamber is made of stainless steel, where the cavity is inside. This furnace equipped with cryopump can reach less than 1×10^{-4} Pa and 1×10^{-6} Pa at 800 °C and room-temperature, respectively, which is favorable for N-doping. During the doping process, nitrogen is injected by a mass flow controller with feedback of a film gauge to stabilize the doping pressure. The performance of this furnace during the doping process is introduced in details. Two 1.3 GHz 1-cell cavities made of fine grain niobium have received N-doping at this furnace, and the vertical test results are promising. The best intrinsic quality factor (Q_0) of these cavities have exceeded 3×10^{10} at 24 MV/m, which is the target of vertical test for Circular Electron Positron Collider (CEPC). Besides, the phenomenon of anti-Q-slope is also obvious. It seems that the stainless steel is harmless to the cavity performance.

1. Introduction

In recent years, researches on N-doping has been carried out widely to improve the intrinsic quality factor (Q_0) of superconducting radio frequency (SRF) cavity [1,2], which has also been adopted as the baseline cavity treatment for Linac coherent light source II (LCLS-II) [3]. After N-doping, Q_0 of 1.3 GHz cavities can reach $\sim4\times10^{10}$, which is more than 2 times as much as before. Therefore, N-doping can reduce the cost of the cryogenic system greatly. In China, Shanghai High repetition rate XFEL and Extreme light facility (SHINE) has begun construction in 2018, which requires 600 1.3 GHz 9-cell cavities with high Q_0. In the future, CEPC adopts a 650 MHz RF system with 240 2-cell cavities for the collider and a 1.3 GHz RF system with 96 9-cell cavities for the booster, which also requires high Q_0 [4]. The 1.3 GHz 9-cell cavities of CEPC are operated at 2 K with $Q_0>3\times10^{10}$ at 24 MV/m for the vertical acceptance test. Hence, research on N-doping has been conducted at IHEP. According to the experience of FNAL and JLab [5,6], the performance of the furnace is key to success of the N-doping. Therefore, a new dual-vacuum furnace was developed at IHEP to obtain higher performance. A lot of N-doping experiments have been carried out with this furnace, and the good results have already been observed.

2. Dual-vacuum furnace at IHEP

2.1. Furnace structure

The new dual-vacuum furnace is designed for 1.3 GHz 1-cell cavities. This furnace, different from the common ones, is equipped with two vacuum systems separately. As shown in Fig. 1, the heater of the furnace is installed in the outer chamber, so the inner chamber will be much cleaner with better vacuum.

The inner chamber is made of stainless steel. It is evacuated by an oil-free scroll roughing pump first, and then the high vacuum is achieved by a cryopump. A Piranic gauge and a cold cathode gauge are adopted for vacuum measurement, which ranges from 1×10^{5} to 5×10^{-7} Pa. Besides, a film gauge is used to monitor the pressure of N_2 during the doping process with the range from 0.1 to 100 Pa. Moreover, a residual gas analyzer (INFICON RGA50) is employed to monitor the composition of the residual gas during the annealing.

The outer chamber is used to install the heater and thermal shield. The heater is made of molybdenum (Mo) which can heat the inner chamber to 1000 °C at maximum. The vacuum of this chamber is evacuated by an oil pump and the pressure is kept less than 0.1 Pa.

* Corresponding author at: Institute of High Energy Physics, Chinese Academy of Sciences, Beijing 100049, China.
** Corresponding author.
E-mail addresses: shapeng@ihep.ac.cn (P. Sha), dongchao@ihep.ac.cn (C. Dong).

https://doi.org/10.1016/j.nima.2021.165080
Received 9 November 2020; Received in revised form 18 January 2021; Accepted 23 January 2021
Available online 27 January 2021

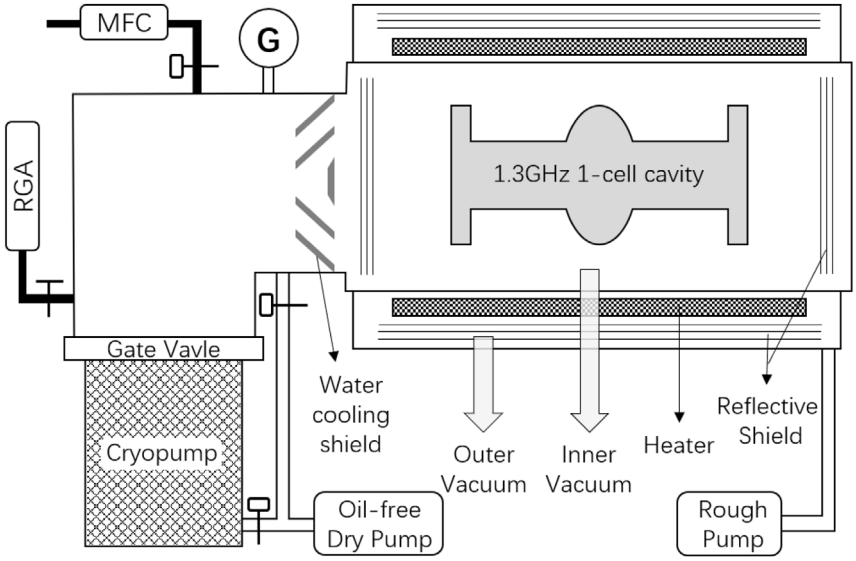

Fig. 1. Structure of the dual-vacuum furnace. The heater is installed in the outer-vacuum chamber, so that the inner-vacuum chamber will be much cleaner with better vacuum.

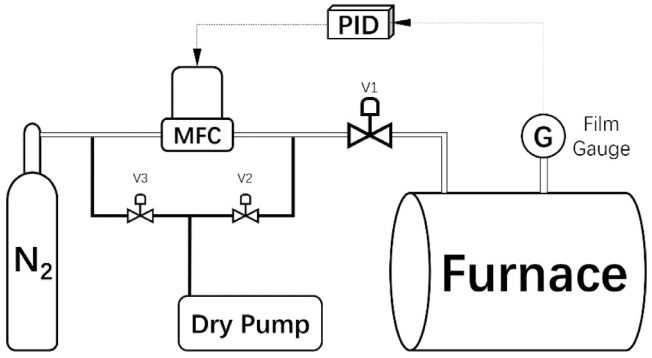

Fig. 2. Nitrogen bleed setup. MFC and a film gauge are used to control the nitrogen flow rate and monitor the nitrogen pressure, the closed-loop feedback can stable the pressure at set point as doping process.

2.2. Nitrogen bleed system

Nitrogen is bled with closed-loop feedback during the doping process. Gas is injected into the furnace through a mass flow controller (MFC), furnace pressure is measured by a film gauge, and a PID algorithm is used to stabilize the pressure at set point.

As shown in Fig. 2, nitrogen comes from the high-pressure gas cylinder, which flows along the stainless-steel pipe to MFC. Next, the gas will be injected into the furnace through an isolation valve (V1). The purity of the nitrogen is the key for the doping process, which is controlled by several methods: (1) the gas in the pipe is replaced by high-purity nitrogen every time after the pipeline is exposed to air; (2) the pipe is baked at 180 °C for 48 h to degas enough; (3) the pipe is always full of high-purity nitrogen with positive pressure, which helps to prevent contamination.

2.3. User interface and operation

The user interface of the furnace is shown in Fig. 3, by which the operator can monitor the furnace status, open valves, turn on pumps and heaters. There are two operation modes: manual and automatic. For the manual mode, the user can actuate the pneumatic valve and pumps by pressing the button on the interface. For the automatic mode, the user needs to set the temperature curve and the PLC of the furnace will execute the commands step by step to complete the total annealing and doping process.

3. N-doping process with the dual-vacuum furnace

3.1. Cavity preparation

Before N-doping, the two 1.3 GHz 1-cell cavities (S8#, S17#) have been treated with different recipes. S8# received bulk EP (100 um), annealing at 750 °C for 3 h, light EP (30 μm), assembly in clean room, low-temperature baking (75 °C 3h + 120 °C 48 h). S17# received bulk EP (180 um), annealing at 950 °C for 3 h, light EP (25 um), assembly in clean room, low-temperature baking (75 °C 3 h + 120 °C 48 h). The vertical test results of EP baseline are shown in Fig. 9. The radiation began increasing at ~34 MV/m for both cavities, which all exceeded the gradient of 40 MV/m. So S8# and S17# were considered qualified for the N-doping followed. In order to remain consistent with S17#, S8# received another annealing at 950 °C for 3 h, followed with light EP (20 μm).

Then, the cavities were transferred to the clean room. The outer surface of cavity was rinsed with Liquinox solution (2%) manually, while the inner surface received high pressure rinse (HPR). When transferred to the furnace, the cavity was supported with two holders made of Niobium. Both flanges of the cavity were covered with Niobium foil, which avoided contaminating deposition on the inner surface and prevented itself from dust. The typical placement of 1.3 GHz 1-cell cavity and some Niobium samples (wrapped by niobium foil) in the furnace is shown in Fig. 4.

3.2. N-doping process

Various N-doping recipes have been tried at this furnace, and the typical process experienced is shown in Fig. 5. Firstly, the furnace is evacuated and pumped until the pressure less than 1×10^{-6} Pa. Secondly, we heat the furnace with ramping up to 800 °C within 4 h. Thirdly, the furnace is kept at 800 °C for 3 h to remove hydrogen. Fourthly, we close the gate valve of the cryopump and start the doping process. The main doping process are as follows: (1) high-purity nitrogen gas is injected into the furnace for 3 min at a nitrogen pressure of around 3.5 Pa; (2) open the gate valve of the cryopump, restart annealing at 800 °C for 60 min. When the doping is finished, the cavity is cooling down naturally to less than 50 °C. The total process has referred to LCLS II HE [7], which was called "3/60" recipe.

During the whole process, the inner vacuum of the furnace is smaller than 2×10^{-4} Pa. When the furnace is cooling down to room temperature, the inner vacuum is reduced to 5×10^{-7} Pa. Simultaneously, the

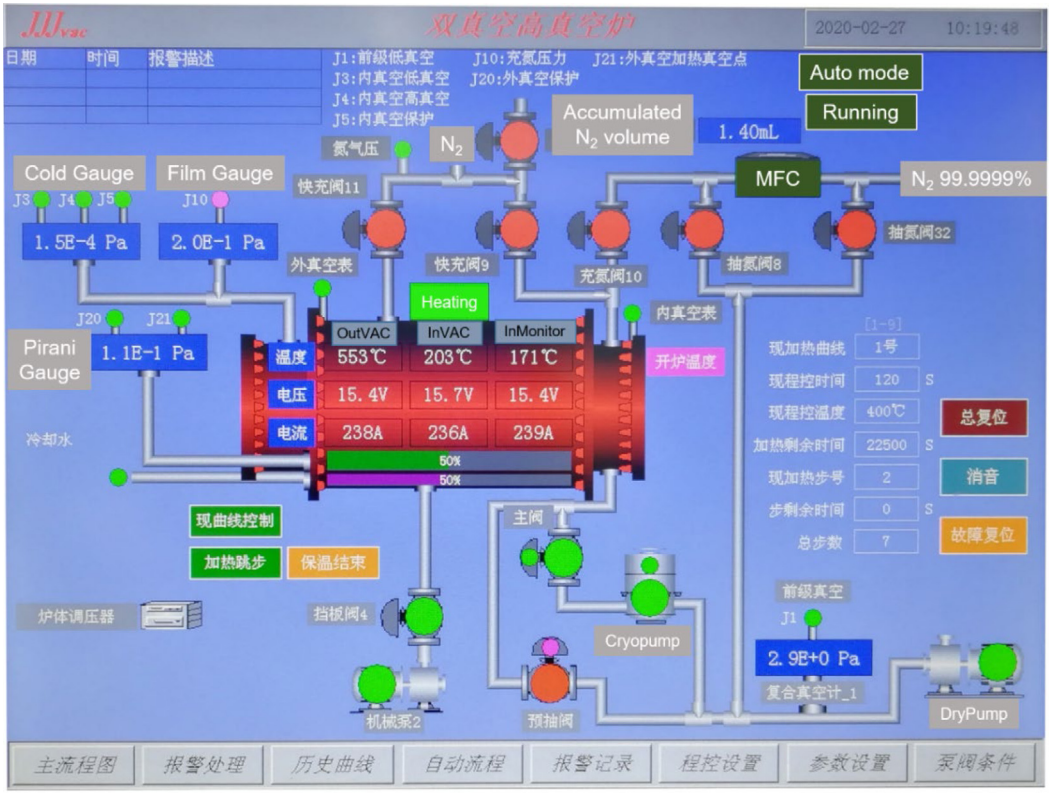

Fig. 3. User interface of the furnace.

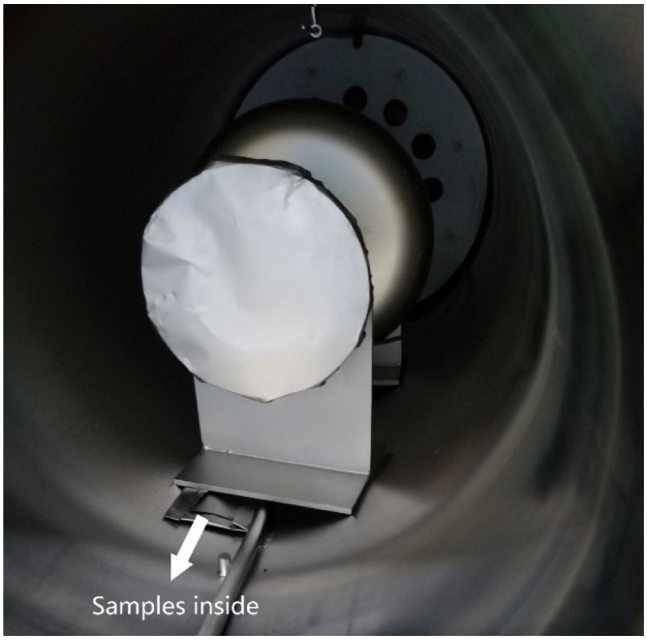

Fig. 4. Placement of a 1.3 GHz 1-cell cavity and some Niobium samples in the inner chamber. The cavity is supported with two holders made of Niobium, and both flanges are covered with Niobium foil. The Niobium samples are wrapped by the same Niobium foil as the cavity.

volume of nitrogen injected is calculated by the flow rate of MFC. In general, one 1.3 GHz 1-cell cavity can absorb about 13~17 scc (Standard-state) nitrogen, of which the value has been subtracted 1.4 scc for the empty furnace.

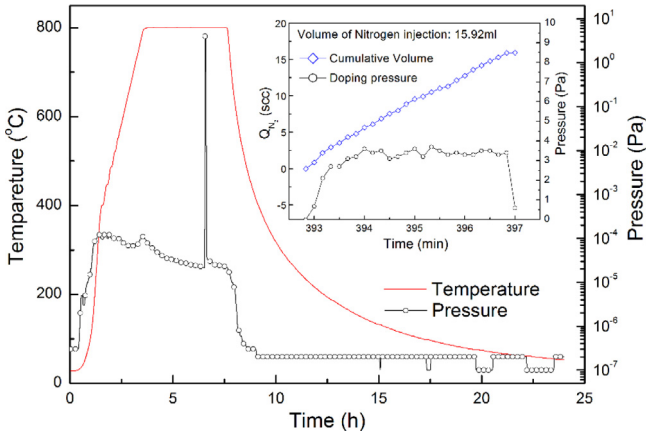

Fig. 5. Variations of temperature and pressure during a typical N-doping process. The inset shows the nitrogen pressure and the cumulative volume of nitrogen absorption during the 3-minutes injection period.

3.3. Analysis of the composition of residual gas

The composition of residual gas in the furnace is monitored by RGA. The six dominant types of gas are hydrogen (Amu 2), water (Amu 18), nitrogen (Amu 28), oxygen (Amu 32), argon (Amu 40), and carbon dioxide (Amu 44). For the 1.3 GHz 1-cell cavity treatment, the evolution of the six types of gas is shown in Fig. 6(a). RGA is shut down to protect the filament during the nitrogen injection. Compared with the empty furnace in Fig. 6(b), it can be found that a large quantity of hydrogen is degassed from the niobium cavity by baking at 800 °C. In addition, there is a higher peak of nitrogen (Amu 28) at the beginning of 800 °C for empty furnace, which indicate nitrogen and carbon monoxide reading from the RGA data (both C and N exist). The

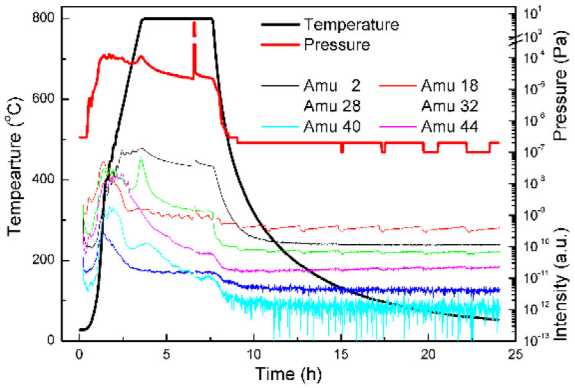

(a) Furnace with a 1.3 GHz 1-cell cavity and samples

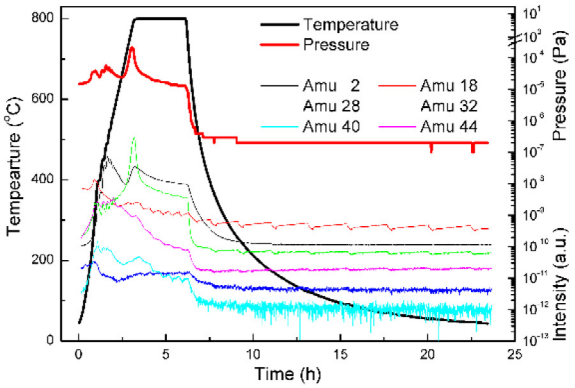

(b) Empty furnace

Fig. 6. Temperature and pressure evolutions of the six dominant types of gas in the furnace during the total doping process. Compared with the empty furnace, more hydrogen is degassed when the niobium cavity is in the furnace.

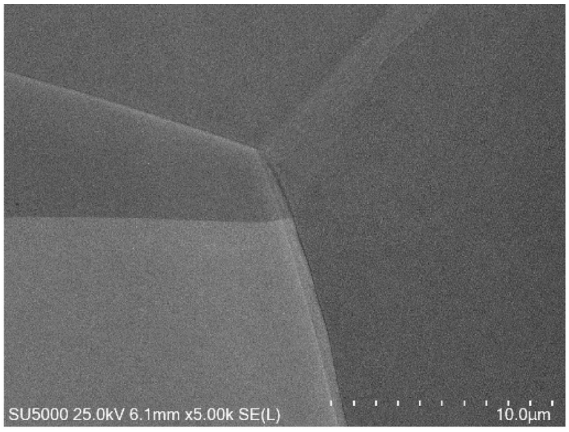

(a) Fine grain Nb sample before N-doping

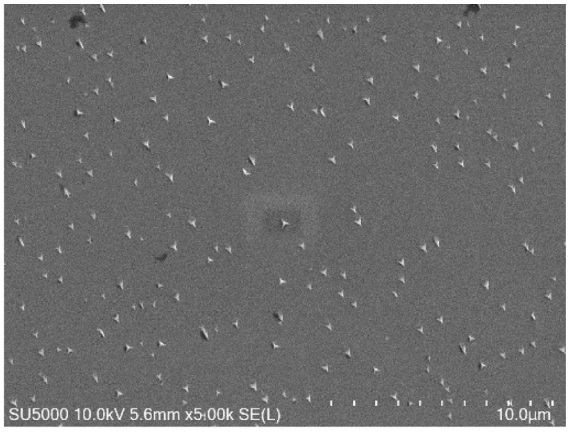

(b) Large grain Nb sample after N-doping

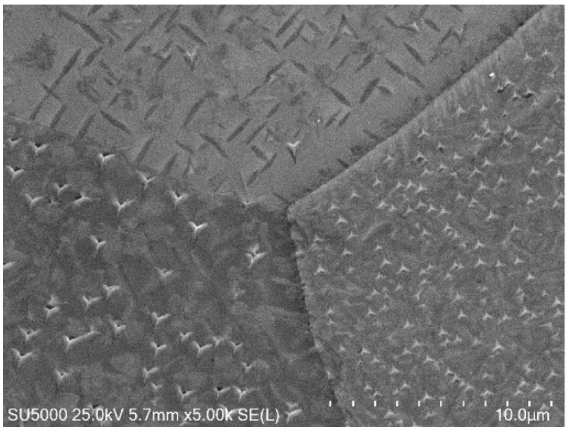

(c) Fine grain Nb sample after N-doping

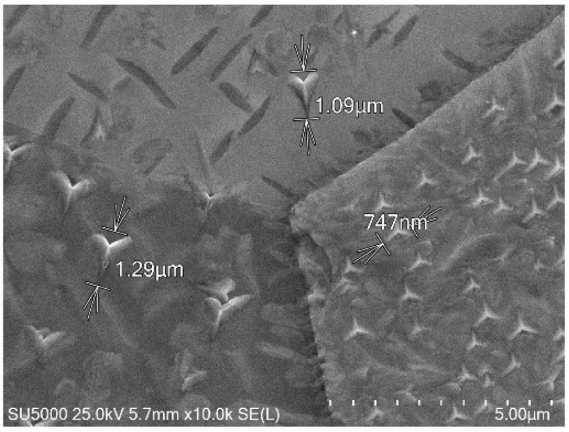

(d) The same fine grain Nb sample as (c) after N-doping at larger magnification to observe surface more clearly

Fig. 7. SEM images of samples, after N-doping, lots of signs with a three-pointed star shape appeared on the sample surface.

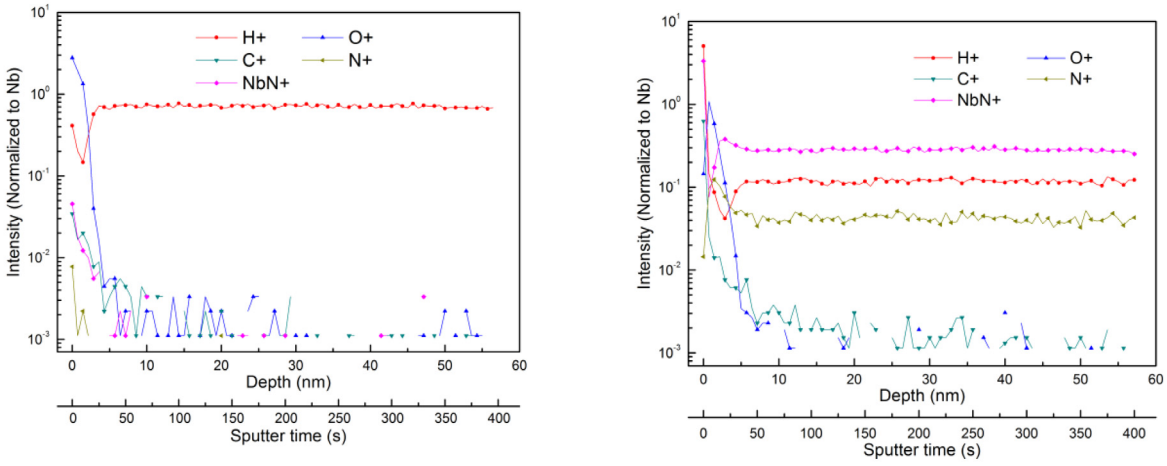

Fig. 8. TOF-SIMS analysis for samples. After N-doping, the concentration of H+ was reduced by one magnitude, while N and NbN diffused into the niobium surface.

same peak is smaller with cavity in the furnace because of the getter pump capacity of niobium.

4. N-doping results

4.1. Sample preparation and analysis

To figure out the N-doping effects, we carried out scanning electron microscope (SEM) [8] and time-of-flight secondary ion mass spectrometry (TOF-SIMS) [9,10] measurements with some Nb samples, which have received N-doping together with the 1.3 GHz 1-cell cavity.

Fig. 7 shows the SEM images of the sample surface. The samples include one fine grain undoped sample, two N-doped samples (one large grain, one fine grain). All samples of sizes 10 mm (W) × 10 mm(L) × 2.8 mm (T) were cut from a high purity Nb (RRR > 300) sheet. And the samples were subjected to the same treatments as the cavity for baseline. By comparing the surface topography between the samples before and after N-doping, it is clear that lots of signs, which represent niobium nitride, with a three-pointed star shape appeared on the sample surface after N-doping, indicating that the nitrogen has reacted with niobium during the doping process. From Fig. 7(b) and (c), there is no grain boundary on the surface of the large grain sample, however, there are obvious grain boundaries on the surface of the fine grain sample. At the same time, the signs appeared irregularly on the large grain sample surface, but the signs have different sizes and orientations for different grains on the fine grain sample surface as shown in Fig. 7(d).

The samples for TOF-SIMS were cut from niobium sheet by Wire Cut Electrical Discharge Machining. They have received annealing of 800 °C 3 h and BCP treatment. The roughness is about 0.77 μm. Before N-doping, samples were cleaned with ethanol again. TOF-SIMS depth profiles indicate the intensities of H^+, N^+, C^+, O^+, and NbN^+ (Y-axis), which are normalized to Nb^+. It is a function of depth from the sample surface (X-axis), with pulsed Bi^+ (30 keV) as analysis gun and Cs^+ (1 keV) as sputter gun. From Fig. 8(a), it is easy to see that for the sample undoped, almost only the concentration of H^+ could extend uniformly to more than 50 nm on the surface, while other ions disappeared quickly within 10 nm from the surface. However, after N-doping, the concentration of H^+ was reduced by one magnitude, while N and NbN diffused into the niobium surface for more than 50 nm. In addition, there is a little more C because of the high-temperature heat treatment.

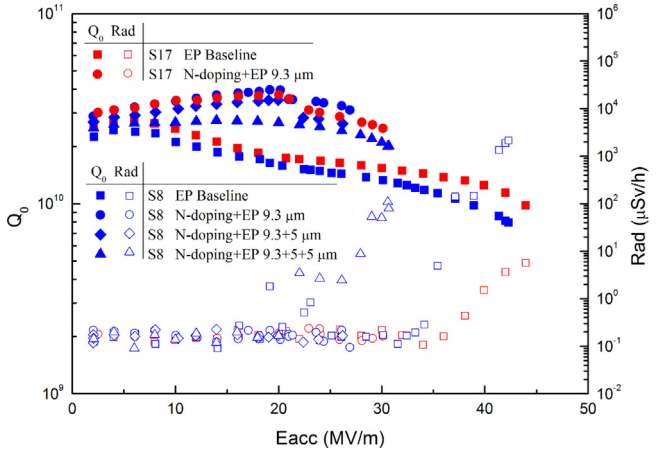

Fig. 9. Vertical test results of two N-doped 1.3 GHz 1-cell cavities.

4.2. Cavity vertical test results

In order to remove the niobium nitride on the inner surface of the cavity, 9.3 μm of light EP was adopted after N-doping. The vertical test results of two 1.3 GHz 1-cell cavities (S8#, S17#) at 2.0 K are shown in Fig. 9. Both cavities demonstrate a much higher Q_0 than EP baseline, which has exceeded the vertical test target (3×10^{10} @ 24 MV/m) for CEPC. Besides, the "anti-Q-slope" phenomenon is also obvious, which showed rising Q_0 versus gradient [11]. No field emission occurred during the vertical tests. However, quench fields of both cavities decrease to < 30 MV/m, compared with > 40 MV/m in the EP baseline test [12].

Moreover, in order to figure out the best removal thickness by EP, S8# received another 5 um of light EP for two times. After the 1st removal of 5 um, the Q_0-E_{acc} curve of S8# is almost the same. The Q_0 decreases after the 2nd removal of 5 um, while the maximum gradient increase. But the Q_0 is still higher than EP baseline obviously, so the effect of N-doping is still residual and more removal is needed to reset the cavity surface. The best removal thickness by EP after N-doping may be 10~ 15 μm, which can achieve balance between high Q_0 and gradient.

5. Conclusion

A new dual-vacuum furnace has been developed to perform N-doping heat treatment on 1.3 GHz 1-cell Niobium cavities at IHEP. This

furnace is equipped with a stainless steel inner chamber and the heater is in the outer vacuum chamber. So the inner vacuum chamber is much cleaner with a better vacuum, which is beneficial for N-doping. MFC with feedback is used for Nitrogen injection during the doping process for monitor the absorption of Nitrogen.

At this furnace, the N-doping process has been carried out on 1.3 GHz 1-cell cavities. The RGA results show that a large quantity of hydrogen is degassed from the niobium cavity by heat treatment with cryopump. SEM and SIMS results of niobium samples indicate that the intensity of hydrogen's decrease and nitrogen's increase in the niobium surface after N-doping process. The vertical test results of both cavities show that the quality factor is significantly improved after N-doping, which have exceeded 3×10^{10} at 24 MV/m.

CRediT authorship contribution statement

Baiqi Liu: Conceptualization, Methodology, Data curation, Writing - original draft, Visualization. **Peng Sha:** Validation, Investigation, Resources, Writing - review & editing, Supervision, Funding acquisition. **Chao Dong:** Data curation, Writing - review & editing. **Feisi He:** Resources. **Weimin Pan:** Project administration. **Zhenghui Mi:** Data curation. **Jiyuan Zhai:** Investigation. **Song Jin:** Methodology. **Jin Dai:** Methodology. **Zhongquan Li:** Investigation. **Lei Du:** Investigation. **Fei Wang:** Data curation. **Liangrui Sun:** Validation. **Rui Ge:** Validation.

Declaration of competing interest

The authors declare that they have no known competing financial interests or personal relationships that could have appeared to influence the work reported in this paper.

Acknowledgments

This work was supported by the National Key Programme for S&T Research and Development (No. 2016YFA0400400), the Platform of Advanced Photon Source Technology R&D, National Natural Science Foundation of China (No. 11505197)

References

[1] A. Grassellino, A. Romanenko, S. Posen, Y. Trenikhina, O. Melnychuk, D.A. Sergatskov, M. Merio, N doping: Progress in development and understanding, in: Proceeding of SRF2015, Whistler, BC, Canada, 2015, pp. 48–54, http://accelconf.web.cern.ch/SRF2015/papers/moba06.pdf.

[2] A. Grassellino, A. Romanenko, D. Sergatskov, O. Melnychuk, Y. Trenikhina, A. Crawford, A. Rowe, M. Wong, T. Khabiboulline, F. Barkov, Nitrogen and argon doping of niobium for superconducting radio frequency cavities: a pathway to highly efficient accelerating structures, Supercond. Sci. Technol. 26 (2013) 102001, http://dx.doi.org/10.1088/0953-2048/26/10/102001, (6pp).

[3] D. Gonnella, S. Aderhold, A. Burrill, E. Daly, K. Davis, A. Grassellino, C. Grimm, T. Khabiboulline, F. Marhauser, O. Melnychuk, A. Palczewski, S. Posen, M. Ross, D. Sergatskov, A. Sukhanov, Y. Trenikhina, K.M. Wilson, Industrialization of the nitrogen-doping preparation for SRF cavities for LCLS-II, Nucl. Instrum. Methods Phys. Res. A 883 (2018) 143–150, http://dx.doi.org/10.1016/j.nima.2017.11.047.

[4] H.J. Zheng, J. Gao, J.Y. Zhai, P. Sha, F.S. He, Z.Q. Li, S. Jin, Z.H. Mi, J.K. Hao, RF design of 650 MHz 2-cell cavity for CEPC collider, Nucl. Sci. Tech. 30 (2019) 155, http://dx.doi.org/10.1007/s41365-019-0671-6.

[5] M. Merio, A. Crawford, A. Grassellino, A. Rowe, M. Wong, M. Checchin, M. Martinello, Furnace N2 doping treatment at Fermilab, in: Proceeding of SRF2015, Whistler, BC, Canada, 2015, pp. 423–427, http://accelconf.web.cern.ch/SRF2015/papers/mopb111.pdf.

[6] A.D. Palczewski, R.L. Geng, C.E. Reece, Analysis of new high-Q0 SRF cavity tests by nitrogen gas doping AT Jefferson Lab, in: Proceeding of LINAC14, Geneva, Switzerland, 2014, pp. 736–739, http://accelconf.web.cern.ch/LINAC2014/papers/tupp138.pdf.

[7] D. Bafia, A. Grassellino, A. Romanenko, M. Checchin, O.S. Melnychuk, D.A. Sergatskov, J.F. Zasadzinski, New insights on nitrogen doping, in: Proceeding of SRF2019, Dresden, Germany, 2019, pp. 347–354, http://accelconf.web.cern.ch/srf2019/papers/tufua4.pdf.

[8] P. Dhakal, G. Ciovati, U. Pudasaini, et al., Surface characterization of nitrogen-doped high purity niobium coupons compared with superconducting rf cavity performance, Phys. Rev. Accel. Beams 22 (2019) 122002, http://dx.doi.org/10.1103/PhysRevAccelBeams.22.122002.

[9] D. Gonnella, S. Aderhold, D. Bafia, A. Burrill1, M. Checchin, M. Ge, A. Grassellino, G. Hays, M. Liepe, M. Martinello, A. Palczewski, S. Posen, T. Raubenheimer, C. Reece4, A. Romanenko, M. Ross, The LCLS-II HE high Q and gradient R & D program, in: Proceeding of SRF2019, Dresden, Germany, 2019, pp. 154–158, http://accelconf.web.cern.ch/srf2019/papers/mop045.pdf.

[10] S. Chen, J.K. Hao, L. Lin, F. Zhu, L.W. Feng, F. Wang, H.M. Xie, X. Guo, M. Chen, S.W. Quan, K.X. Liu, Successful nitrogen doping of 1.3 GHz single cell superconducting radio-frequency cavities, Chin. Phys. Lett. 35 (3) (2018) 037401, http://dx.doi.org/10.1088/0256-307X/35/3/037401.

[11] M. Martinello, N-doping: A breakthrough technology for SRF cavities, in: Proceeding of LINAC2016, East Lansing, Michigan, USA, 2016, http://accelconf.web.cern.ch/linac2016/talks/we2a01_talk.pdf.

[12] D. Gonnella, S. Aderhold, A. Burrill, E. Daly, K. Davis, A. Grassellino, C. Grimm, T. Khabiboulline, F. Marhauser, O. Melnychuk, A. Palczewski, S. Posen, M. Ross, D. Sergatskov, K. Wilson, RF performance of nitrogen-doped production SRF cavities for LCLS-II, in: Proceedings of IPAC2017, Copenhagen, Denmark, 2017, pp. 1156–1159, http://accelconf.web.cern.ch/ipac2017/papers/mopva128.pdf.